Computational and Mathematical Methods in Medicine
Vol. 9, Nos. 3–4, September–December 2008, 221–229

Taylor & Francis
Taylor & Francis Group

New insights into viral architecture via affine extended symmetry groups

T. Keef[a1] and R. Twarock[b]*

[a]*Department of Mathematics, University of York, York, UK;* [b]*Department of Biology, University of York, York, UK*

(*Received 2 April 2008; final version received 28 April 2008*)

Since the seminal work of Caspar and Klug on the structure of the protein containers that encapsulate and hence protect the viral genome, it has been recognized that icosahedral symmetry is crucial for the structural organization of viruses. In particular, icosahedral symmetry has been invoked in order to predict the surface structures of viral capsids in terms of tessellations or tilings that schematically encode the locations of the protein subunits in the capsids. Whilst this approach is capable of predicting the relative locations of the proteins in the capsids, a prediction on the relative sizes of different virus particles in a family cannot be made. Moreover, information on the full 3D structure of viral particles, including the tertiary structures of the capsid proteins and the organization of the viral genome within the capsid are inaccessible with their approach. We develop here a mathematical framework based on affine extensions of the icosahedral group that allows us to address these issues. In particular, we show that the relative radii of viruses in the family of Polyomaviridae and the material boundaries in simple RNA viruses can be determined with our approach. The results complement Caspar and Klug's theory of quasi-equivalence and provide details on virus structure that have not been accessible with previous methods, implying that icosahedral symmetry is more important for virus architecture than previously appreciated.

Keywords: viral capsids; affine extensions; icosahedral symmetry; tilings

1. Introduction

An important constituent of a virus is its protein container called the viral capsid, that packages the genomic RNA or DNA. Crick and Watson observed in 1956 that the size of the packaged genomic material is too small to encode for more than a limited number of different capsid proteins. Based on this observation they argued that viruses must be formed from identical capsid proteins that are organized according to symmetry [2]. Subsequent experiments confirmed this conjecture, showing that most viruses exhibit icosahedral symmetry. Since the number of identical proteins in identical locations in a capsid exhibiting symmetry equals the order of the corresponding symmetry group, and since the icosahedral group is the finite group in 3D of largest order (order 60), this predominance of icosahedral symmetry in virus architecture is a logical consequence of sequence economy in the viral genome. Icosahedral symmetry alone, however, cannot explain the surface structures of viral capsids with more than 60 capsid proteins. Therefore, Caspar and Klug introduced the concept of quasi-equivalence, which states that capsid proteins must be organized such that their local environments are 'almost equivalent'. From a mathematical point of view, they realized this concept by classifying viral capsids in terms of triangulations with overall icosahedral symmetry and their approach predicts that viral capsids are organized in terms of 12 clusters of 5 proteins (pentamers) and 10 ($T - 1$)

*Corresponding author. Email: rt507@york.ac.uk

ISSN 1748-670X print/ISSN 1748-6718 online

DOI: 10.1080/17486700802168163
http://www.informaworld.com

clusters of 6 proteins (hexamers), where T called the T-number, takes on any value $h^2 + hk + k^2$ with $h, k \in \mathbb{N}$ [1].

Caspar–Klug theory has become a fundamental concept in virology with a plethora of applications, including the reconstruction of capsid shapes from experimental data and their classification. However, experiments concerning the cancer-causing Papovaviridae have shown that there are viruses that do not follow the organization predicted by this theory [16,19]. In particular, these viruses are formed from pentamers throughout – for example 72 pentamers in the case of human papilloma virus – and their surface structures can hence not be described via triangulations. It has been shown in Refs. [14,28,29] that Caspar–Klug Theory can be generalized to incorporate these cases by considering not only lattice structures, but also quasi-lattices as known from the study of quasi-crystals [22], *i.e.* alloys with atomic arrangements exhibiting long-range order, but no periodicity [23]. A common feature of Caspar–Klug theory and its generalizations is the fact that they use icosahedral symmetry as the maximal symmetry content in the theory and therefore, describe viral capsids schematically in terms of surface lattices or tessellations, rather than as objects extended in space. As a consequence, the predictive power of these theories is limited to specifying the locations and types of the protein clusters in the capsids, their relative orientations and as in the case of the tiling approach, the locations of the bonds between the capsid proteins. Information on the tertiary structures of the capsid proteins, the thickness of the capsid and the organization of the genomic material, or on the relative sizes of different particles in a family is inaccessible.

In this paper, we show that there is more symmetry present in the organization of viruses than presently appreciated. It is known – for example from the study of nested carbon cage structures called carbon onions [27] – that the symmetry of an extended structure exhibiting a certain compact symmetry (such as icosahedral symmetry) at different radial levels can be described by an affine extension of this symmetry group. Analogous to this, we aim here at describing the full 3D structures of viruses, *i.e.* the organization of material at different radial levels *collectively*, as well as different particles in the same family of viruses *collectively* in terms of affine extensions of the icosahedral group. Such an approach is further motivated by work of Janner [6–8], which shows that lattice-like structures obtainable from a higher-dimensional lattice with icosahedral symmetry via projection are relevant for the description of proteins [5–8] or protein assemblies such as viral capsids [9,10]. This is a very important result, but cannot predict which subsets of lattice points are relevant for virus architecture. We present here a method based on affine extensions of non-crystallographic Coxeter groups, most notably of the reflection group H_3, that contains the rotational symmetries of the icosahedron as a subgroup and specifies finite subsets of such quasi-lattices relevant for virus structure prediction. This construction principle is similar to the construction of lattices from symmetry groups (space groups), but leads to lattice-like, rather than lattice, structures due to the non-crystallographic nature of the underlying symmetry group.

This paper is organized as follows: In Section 2.1, we review a standard approach for affine extensions and show how it can be applied in virology for the prediction of the size spectrum of different particles in the family of Polyomaviridae. In Section 3, we discuss the limitations of this approach and encorporate it into a broader framework that leads to suitable group theoretical objects for the prediction of 3D virus architecture.

2. Affinization of non-crystallographic Coxeter groups and assembly polymorphism

In this section, we first review a standard construction method for patches of quasi-lattices with icosahedral symmetry following [17]. We then discuss the implications of these results for the

modelling of Polyomaviridae assembly polymorphism and infer predictions on the sizes of different particles occurring during *in vitro* assembly of the major capsid protein in that family.

2.1. A standard approach for the affinisation of a non-crystallographic Coxeter group

With applications to viruses in mind, we are looking for mathematical objects that describe an extended structure with overall icosahedral symmetry and predict how icosahedral symmetry is realized at different radial levels. We consider the non-crystallographic Coxeter group H_3 [4], because it contains the rotational symmetries of the icosahedral group as a subgroup and determine ways of extending this finite group into an infinite one by addition of a non-compact generator such as a translation. By acting with such an affine extended symmetry group on a seed configuration, patches of quasi-lattices are obtained as demonstrated in Figure 1.

Only a few distinguished translations are suitable if these point sets are supposed to have properties relating them to quasi-lattices (or icosahedral lattices in the sense of Janner [6], because each quasi-lattice point can be obtained via projection from a crystallographic lattice in six dimensions). One-way of obtaining such a suitable translation T is via the Kac-Moody formalism (see Ref. [17] and references within for details). The affine extended group H_3^{aff} obtained in this way is given by the elements of H_3 and T. An iterative application of the group generators of the extended group to a start vector v generates point sets $\mathcal{S}(k)$, which correspond to all group generators expressible in terms of at most k copies of T acting on v. These sets become increasingly dense and extended in space with increasing k as shown for $k = 1, 2, 3$ in Figure 2.

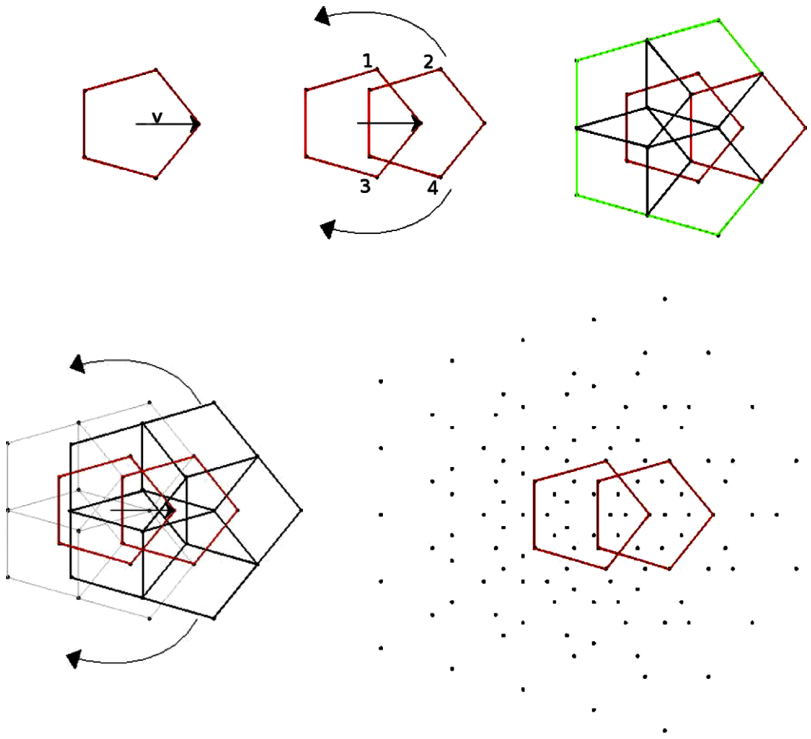

Figure 1. The construction method illustrated for a 2D example. The symmetry group is given by the rotational symmetries of the pentagon. Together with the translation, the generators of the rotational symmetry group generate copies of the original pentagon in space. The vertices of these pentagons form a point set that has the properties of a quasi-lattice [17]. Available in colour online.

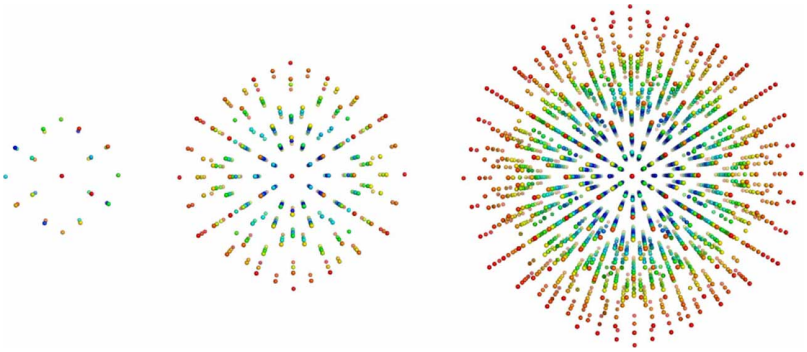

Figure 2. The point sets $\mathcal{S}(k)$ for $k = 1, 2, 3$. Available in colour online.

2.2. *Applications to Polyomaviridae*

Viral tiling theory [28,29] shows that the surface structures of viruses can be encoded in terms of tilings that encode the locations of the capsid proteins and the dominant bonds between them. In this section, we search for tilings with vertices in the point set $\mathcal{S}(k)$ for suitable k that may represent the three particles observed during Polyomavirus assembly. We choose k as the minimal integer such that the surface structures of all viral particles in a family are collectively encoded by vertices in that set; for Polyomaviridae, we obtain $k = 5$. We have computed the set $\mathcal{S}(5)$ explicitly: The points are organized on 181 nested shells of radii between $r_1 \approx 0.2361$ and $r_2 = 5$. In order to locate the subsets of $\mathcal{S}(5)$ that contain the vertices of the tilings corresponding to viral particles in the family of Polyomaviridae, we have searched for vertices that correspond to the observed locations of the capsomeres (*i.e.* the clusters of capsid proteins) in each case. We have obtained the following results [14], which are illustrated in Figure 3:

- *The small particle*: These particles are represented by icosahedra with vertices on the 5-fold axes of icosahedral symmetry and are located at radius $r \approx 1.176$.
- *The medium-size particle*: These particles are represented by tilings with vertices at the 3-fold axes on radius $r_M \approx 1.732$ and at the 4-fold axes on radius $r = 2$. The locations of the pentamers are at $r \approx 1.940$. The proteins are located in the corners of the tiles meeting at the 24 five-coordinated vertices, hence, specifying locations and orientations of the 24 pentamers.
- *The large particle*: The tiling for the large particle contains vertices at the 3-fold axes at $r_L \approx 2.803$. The 12 pentamers on the 5-fold axes of icosahedral symmetry appear on radius $r \approx 3.078$, whereas the remaining 60 pentamers off the symmetry axes of icosahedral symmetry occur on radii $r = 3$ and $r \approx 2.786$, with $r = 3$ marking the pentavalent vertices defining the pentamers and $r \approx 2.976$ the trivalent vertices needed to complete the tiling.

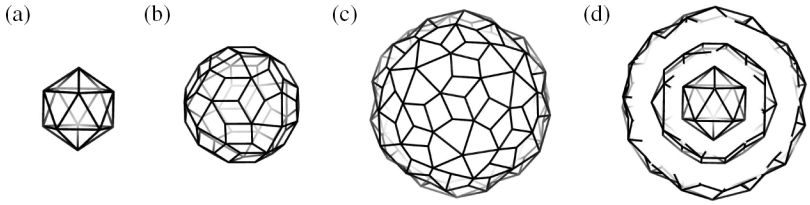

Figure 3. The tilings representing the three types of particles: (a) the small, (b) the medium-size and (c) the large particle. (d) All three tilings shown in relative location as implied by their vertices in $\mathcal{S}(5)$.

Note that the medium-size and large particle are not isometric, even though the deviations are small and might not easily be detectable experimentally. Since the surface lattices have been determined as subsets of the same set $\mathcal{S}(5)$, the sizes of the three different types of particles are fixed in relation to each other as shown in Figure 3(d). There is hence *only one free parameter* that relates the overall mathematical structure, *i.e.* the surface lattices of all particles *collectively*, to the biological setting. This factor has been computed in Ref. [14] and has been shown to be in excellent agreement with the experimental data in Ref. [11,21].

3. Generalizations: Affine extended symmetry systems

The affine extensions obtained in the previous section constitute only one way of associating mathematically meaningful translations with the generators of the icosahedral group and so, it is not surprising that they are not sufficient to describe all viruses. However, their properties are representative of those of the mathematical structures needed for applications in virology. In particular, the key property of these translations is the fact that there are coinciding elements in the monomial set of the extended symmetry group when applied to a start configuration. This property manifests itself in identities such as that the vertex denoted 2 can be obtained in two ways in Figure 1, *i.e.* $2 = TRv = RTR^4v$, with R a rotation about the origin of $2\pi/5$. The generalization hence depends on the choice of a vector v that serves as a 'start vector'. From a geometric point of view, the structure of the translation that complements the generators of the symmetry group in the affine extension hence, depends on a representation of the symmetry group, which can be encoded by a *start configuration* S that is obtained from the start vector via the action of the symmetry group G, *i.e.* $S = Gv$. Due to this dependence on the geometric realization of the symmetry group, we introduce the concept of a *symmetry system* (G, S), given by a symmetry group G and a start configuration S. Since the formalism employed in the previous section does not consider this, the affine extensions obtained for symmetry systems represent mathematical objects that are more general than those obtained via the standard formalism and they indeed incorporate the translations obtained via the standard formalism as a special case.

For the icosahedral group there are three start configurations that are distinguished by set economy. These are given by the icosahedron, the dodecahedron and the icosidodecahedron, shown in Figure 4, and have vertices on the 5-, 3- or 2-fold axes of icosahedral symmetry, respectively.

The translations along symmetry axes for the symmetry systems given by the icosahedral group and any of these start configurations have been determined in Ref. [12]. It has been shown that there are precisely 54 such translations. Table 1 summarizes these results and indicates the translations associated with each start configuration. Translations are given in terms of $\tau = (1/2)(1 + \sqrt{5})$, $\tau' = (1/2)(1 - \sqrt{5})$ and the unit translation vectors $\vec{T}_j, j \in \{2, 3, 5\}$ along axes of 2-, 3- and 5-fold symmetry. Each translation in the Table defines an affine extended symmetry group, and each such symmetry group, when applied to an element in the start configuration, defines point sets analogous

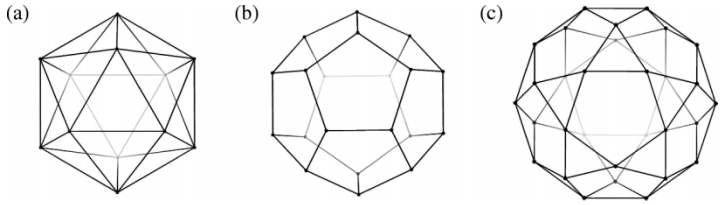

Figure 4. The icosahedron (a), dodecahedron (b) and icosidodecahedron (c) corresponding to the three distinguished start configurations.

Table 1. The cardinalities of the lattice-like point sets generated from the 54 extended symmetry systems.

Icosahedron		Dodecahedron		Icosidodecahedron	
Translation	Cardinality	Translation	Cardinality	Translation	Cardinality
$-\tau'\vec{T}_5$	116	$\tau'2\vec{T}_5$	200	$-(1/2)\tau'\vec{T}_5$	290
$\vec{T}_5$	85	$-\tau'\vec{T}_5$	172	$(1/2)\vec{T}_5$	242
$\tau\vec{T}_5$	116	$\vec{T}_5$	172	$(1/2)\tau\vec{T}_5$	242
		$\tau\vec{T}_5$	200	$\vec{T}_5$	360
				$(1/2)\tau^2\vec{T}_5$	290
				$\tau\vec{T}_5$	360
$-\tau'\vec{T}_3$	192	$-(1/2)\tau'\vec{T}_3$	360	$-(1/2)\tau'\vec{T}_3$	510
$\vec{T}_3$	164	$-\tau'\vec{T}_3$	252	$(1/2)\vec{T}_3$	362
$\tau\vec{T}_3$	164	$\vec{T}_3$	191	$(1/2)\tau\vec{T}_3$	374
$\tau^2\vec{T}_3$	192	$\tau\vec{T}_3$	252	$\vec{T}_3$	600
				$(1/2)\tau^2\vec{T}_3$	362
				$\tau\vec{T}_3$	570
				$(1/2)\tau^3\vec{T}_3$	510
				$\tau^2\vec{T}_3$	600
$-\tau'\vec{T}_2$	342	$\tau'2\vec{T}_2$	590	$-(1/2)\tau'\vec{T}_2$	870
$2\tau'2\vec{T}_2$	272	$-2\tau'3\vec{T}_2$	500	$\tau'2\vec{T}_2$	710
$\vec{T}_2$	342	$-\tau'\vec{T}_2$	560	$(1/2)\vec{T}_2$	870
$-2\tau'\vec{T}_2$	212	$2\tau'2\vec{T}_2$	332	$-\tau'\vec{T}_2$	552
$2\vec{T}_2$	212	$\vec{T}_2$	590	$\tau/2\vec{T}_2$	870
$2\tau\vec{T}_2$	272	$-2\tau'\vec{T}_2$	344	$\vec{T}_2$	361
		$2\vec{T}_2$	332	$-2\tau'\vec{T}_2$	870
		$2\tau\vec{T}_2$	500	$\tau\vec{T}_2$	552
				$2\vec{T}_2$	840
				$\tau^2\vec{T}_2$	710
				$2\tau\vec{T}_2$	870

to Section 2.1 (compare with Figure 1). The new approach to affine extensions of the icosahedral group based on symmetry systems has hence augmented the library of relevant point configurations to 54. We display three elements of this library in Figure 5. These point sets have different cardinalities, *i.e.* different numbers of distinct elements, and we list the cardinalities of all 54 point sets in Table 1. Moreover, affine extensions can be constructed with twist-translations and a classification of this case analogous to the above is presented in Ref. [13].

3.1. Applications to simple RNA viruses

As before we use these point sets in order to characterize virus architecture. In this section, the aim is to predict the material boundaries in simple viruses. Therefore, we iterate the point sets

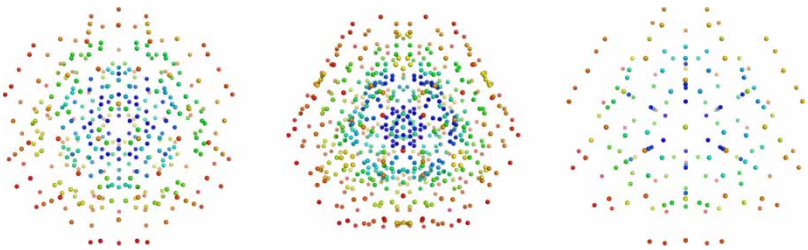

Figure 5. Examples showing three of the 54 configurations in Table 1. Available in colour online.

until enough (by number) layers of points are present to account for all material boundaries. Since we focus on RNA viruses of a relatively small size here, this number is small and we only consider the 54 point configurations in the preceding section and combinations thereof. In particular, combination of two start configurations are possible if they have been obtained via a translation along the same symmetry axis. In this case, we rescale one of the start configurations such that both translation lengths match and then use both start configurations superimposed as a new start configuration in combination with this translation length.

We have applied this increased library to a number of viruses of different structure and sizes [15]: Pariacoto virus, an insect virus with a quasi-equivalent $T = 3$ structure [25], bacteriophage MS2, a quasi-equivalent $T = 3$ phage [3,26,31,32], Satellite Tobacco Necrosis Virus (STNV), a $T = 1$ virus [30] and Poliovirus [24]. In each of the cases, we gauge the biological setting to the outer layer of points in the point configuration, and then infer predictions on internal features. For example, this approach could be used to predict the RNA organization within the viruses we considered. For example, for Pariacoto virus, only three of the 49 classified symmetry systems show reasonable matches. These correspond to the red, blue and green vertices in Figure 6 shown superimposed on the crystal structure of Pariacoto virus which is available as a pdb-file (pdb-ID 1F8V) from the VIPER website [20]. A simple visual comparison shows that whilst, the red dots are located on the most radial distant features of the capsid proteins, the green and blue dots do not fit in a meaningful way with the structure. This demonstrates that discrimination between the different lattice structures is feasible by eye; however, we have performed an RMSD analysis (see Ref. [15]) in each case to quantify this. In a next step, we have to consider all point sets with combined start configurations that have an outer layer of points coinciding with the one we have identified. In the case of Pariacoto virus there are 12 such configurations. We apply the scaling factor associated with the outer layer, *i.e.* the red points in Figure 6, to all other symmetry related points in these 12 configurations and compare with the data. For only one of them, we find a spread of points that remarkably fits around all molecular boundaries of Pariacoto virus. This implies that this virus has assembled to maximize symmetry in 3D and that icosahedral symmetry occurs on different radial levels ochestrated by the new symmetry principle described here. A more extensive analysis of where these points are situated with respect to the molecular components of this and other viruses will be discussed in Ref. [15], where we also show that this approach predicts the organization of the viral RNA within other viruses and phages.

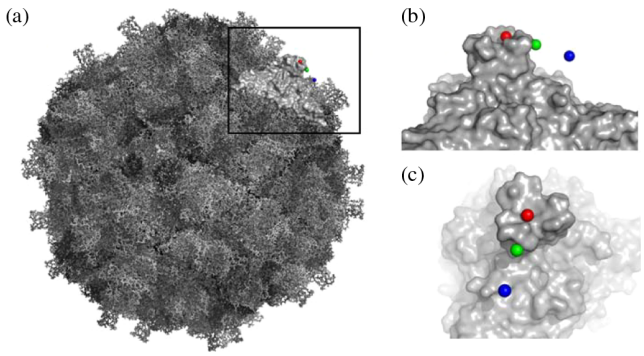

Figure 6. (a) The crystal structure of Pariacoto virus with a trimer highlighted in the upper right-hand corner. (b) and (c) showing close-ups of that trimer, with red points corresponding to the model identified as the outer layer for Pariacoto virus. The green and blue points represent symmetry systems with outer layers closest to the red points; a comparison with the data shows that these are not suitable for the description of Pariacoto virus. Available in colour online.

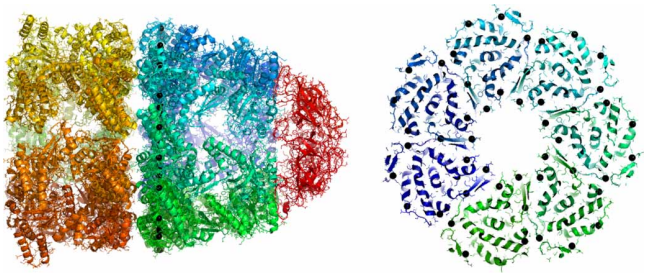

Figure 7. Points with 7-fold symmetry predicting organization of proteins within a slice of the GroEL–GroES protein complex. Available in colour online.

4. Discussion

This analysis suggests that symmetry is more important for virus architecture than previously appreciated. Remarkbly, all viruses we have investigated to date follow the blueprints derived here. This begs the question in how far this new approach consitutes a new general principle in virus architecture. The library of lattice-like structures used in Ref. [15] relies on two assumptions: the overall icosahedral symmetry of the object under consideration and the fact that the viruses and phages under consideration have a number of material boundaries in a certain range. However, the formalism is easily generalizable to situations where these assumptions are violated. For example, we expect that for larger viruses, a suitable library of lattice-like structures can be obtained from the same symmetry systems by considering higher order monomials (larger iteration numbers for T in the expressions of the group generators applied to the start vector). Moreover, for viruses or phages with prolate capsids, where only a reduced symmetry is present (one 5-fold axis only, which reduces the symmetry from icosahedral symmetry 5–3–2 to the subgroup encoding 5-fold symmetry), the same formalism can be applied to the reduced group structure.

Finally, if this principle is of general relevance, one would expect that it has applications also in areas other than virology. We have therefore applied our formalism to another protein complex, GroEL–GroES [18], a cavity with 7-fold symmetry. Also for this case, preliminary results show that our method makes predictions on the three-dimensional organization of the proteins (Figure 7). These results suggest that the new principle presented here is indeed of general relevance in microbiology.

Acknowledgements

RT has been supported by an EPSRC Advanced Research Fellowship. TK has been supported by the EPSRC Grant GR/T26979/01.

Note

1. Email: tk506@york.ac.uk

References

[1] D.L.D. Caspar and A. Klug, *Physical principles in the construction of regular viruses*, Cold Spring Harbor Sympos. Quant. Biol. 27 (1962), pp. 1–24.
[2] F.H.C. Crick and J.D. Watson, *The structure of small viruses*, Nature 177 (1956), pp. 473–475.
[3] R. Golmohammadi, K. Valegard, K. Fridborg, and L. Liljas, *The refined structure of bacteriophage MS2 at 2.8 Å resolution*, J. Mol. Biol. 3 (1993), pp. 620–639.

[4] J.E. Humphreys, *Reflection Groups and Coxeter Groups, Cambridge Studies in Advanced Mathematics*, Vol. 29, Cambridge University Press, Cambridge, 1992.
[5] A. Janner, *Polygrammal symmetries in biomacromolecules: Heptagonal poly d(As^{4}T) poly d(As^{4}T) and heptameric α-Hemolysin*, Struct. Chem. 13 (2002), pp. 277–287.
[6] ———, *Strongly correlated structure of axial-symmetric proteins. I. Orthorhombic, tetragonal, trigonal and hexagonal symmetries*, Acta Crystallogr. D 61 (2005), pp. 247–255.
[7] ———, *Strongly correlated structure of axial-symmetric proteins. II. Pentagonal, heptagonal, octagonal, nonagonal and ondecagonal symmetries*, Acta Crystallogr. D 61 (2005), pp. 256–268.
[8] ———, *Strongly correlated structure of axial-symmetric proteins. III. Complexes with DNA/RNA*, Acta Crystallogr. D 61 (2005), pp. 269–277.
[9] ———, *Crystallographic structural organization of human rhinovirus serotype 16, 14, 3, 2 ans 1a*, Acta Crystallogr. A 62 (2006), pp. 270–286.
[10] ———, *Towards a classification of icosahedral viruses in terms of indexed polyhedra*, Acta Crystallogr. A 62 (2006), pp. 319–330.
[11] S.N. Kanesashi, K. Ishizu, M.A. Kawano, S.I. Han, S. Tomita, H. Watanabe, K. Kataoka, and H. Handa, *Simian virus 40 vp1 capsid protein forms polymorphic assemblies* in vitro, J. Gen. Virol. 84 (2003), pp. 1899–1905.
[12] T. Keef and R. Twarock, *Affine extensions of the icosahedral group with applications to the three-dimensional organisation of simple viruses*, Submitted to J. Math. Biol. (2007).
[13] ———, *Affine extensions of the icosahedral group by translations with a twist: The case of poliovirus*, in preperation (2008).
[14] T. Keef, R. Twarock, and K.M. ElSawy, *A new series of polyhedra as blueprints for viral capsids in the family of Papovaviridae*, J. Theor. Biol. (2007), to appear.
[15] T. Keef, K. Toropova, N.A. Ranson, P.G. Stockley, and R. Twarock, A new paradigm for symmetry reveals hidden features in the architecture of simple viruses in preperation (2007).
[16] R.C. Liddington, Y. Yan, J. Moulai, R. Sahli, T.L. Benjamin, and S.C. Harrison, *Structure of simian virus 40 at 3.8-Å resolution*, Nature 354 (1991), pp. 278–284.
[17] J. Patera and R. Twarock, *Affine extensions of noncrystallographic Coxeter groups and quasicrystals*, J. Phys. A 35 (2002), pp. 1551–1574.
[18] N. Ranson, G.W. Far, A.M. Roseman, B. Gower, W.A. Fenton, A.L. Horwich, and H.R. Saibil, *ATP-bound states of GroEL captured by cryo-electron microscopy*, Cell 107 (2001), pp. 869–879.
[19] I. Rayment, T. Baker, D.L.D. Caspar, and W.T. Murakami, *Polyoma virus capsid structure at 22.5 Å resolution*, Nature 295 (1982), pp. 110–115.
[20] V.S. Reddy, H.A. Giesing, R.T. Morton, A. Kumar, C.B. Post, C.L. Brooks III, and J.E. Johnson, *Virus particle explorer (VIPER), a website for virus capsid structures and their computational analyses*, J. Virol. 75 (2001), pp. 11943–11947.
[21] D.M. Salunke, D.L.D. Caspar, and R.L. Garcea, *Polymorphism in the assembly of Polyomavirus capsid protein VP1*, Biophys. J. 56 (1989), pp. 887–900.
[22] M. Senechal, *Quasicrystals and Geometry*, Cambridge University Press, Cambridge, 1996.
[23] D. Shechtman, I. Blech, D. Gratias, and J.W. Cahn, *Metallic phase with long-range order and no translational symmetry*, Phys. Rev. Lett. 53 (1984), pp. 1951–1953.
[24] R. Syed, D. Filman, and J. Hogle, *Refinement of the Sabin strain of type 3 Poliovirus at 2.4 Angstroms and the crystal structures of its variants at 2.9 Angstroms resolution*, PDB ID 1pvc (1995).
[25] L. Tang, K.N. Johnson, L.A. Ball, T. Lin, M. Yeager, and J.E. Johnson, *The structure of Pariacoto virus reveals a dodecahedral cage of duplex RNA*, Nat. Struct. Biol. 1 (2001), pp. 77–83.
[26] K. Toropova, G. Basnak, R. Twarock, P.G. Stockley, and N.A. Ranson, *The three-dimensional structure of genomic RNA in bacteriophage MS2: Implications for assembly*, J. Mol. Biol. 375 (2008), pp. 824–836.
[27] R. Twarock, *New group structures for carbon onions and carbon nanotubes via affine extensions of noncrystallographic Coxeter groups*, Phys. Lett. A 300 (2002), pp. 437–444.
[28] ———, *A tiling approach to virus capsid assembly explaining a structural puzzle in virology*, J. Theor. Biol. 226 (2004), pp. 477–482.
[29] ———, *The architecture of viral capsids based on tiling theory*, J. Theor. Med. 6 (2005), pp. 87–90.
[30] T. Unge, L. Liljas, B. Strandberg, I. Vaara, K.K. Kannan, K. Fridborg, C.E. Nordman, and P.J. Lentz Jr., *Satellite tobacco necrosis virus structure at 4.0 Å resolution*, Nature 285 (1980), pp. 373–377.
[31] K. Valegard, J.B. Murray, P.G. Stockley, N.J. Stonehouse, and L. Liljas, *The three-dimensional structure of the bacterial virus MS2*, Nature 6270 (1990), pp. 36–41.
[32] ———, et al., *Crystal structure of an RNA bacteriophage coat protein operator complex*, Nature 623 (2002), p. 626.